Evidence of a Hybridization Gap in "Semimetallic" InAs/GaSb Systems

M. J. Yang,[1] C. H. Yang,[2] B. R. Bennett,[1] and B. V. Shanabrook[1]
[1]*Naval Research Laboratory, Washington, D.C. 20375*
[2]*University of Maryland, College Park, Maryland 20742*
(Received 25 November 1996)

InAs/GaSb composite quantum wells sandwiched by AlSb are studied by using capacitance-voltage, quantum Hall, and three-terminal transfer measurements. Our data reveal a positive energy gap resulting from the hybridization of in-plane dispersions of electrons in InAs and holes in GaSb for conventionally recognized "semimetallic" InAs/GaSb heterostructures. [S0031-9007(97)03348-6]

PACS numbers: 71.20.Nr, 72.80.Ey, 73.20.Dx, 73.61.Ey

Semimetals and semiconductors are two different solid state materials. The major property distinguishing these two classes is the energy gap (E_g); i.e., $E_g > 0$ for semiconductors, while $E_g \leq 0$ for semimetals. It has been commonly believed for almost two decades that InAs/GaSb superlattices undergo a semiconductor-to-semimetal transition [1] when the InAs well thickness is increased to a critical value in the vicinity of 85 Å [1,2]. However, self-consistent calculations performed for InAs/GaSb superlattices [3] and quantum wells [4,5] show a hybridization gap of a few meV owing to the coupling between electrons in the InAs well and holes in the GaSb well. Although there are several magneto-optical [6–8] and magnetotransport [9] works which show the impact of electron-hole hybridization on the data, there has never been conclusive measurement of the hybridization gap. As a result, the term "semimetallic InAs/GaSb" still prevails in the scientific community. In this Letter we provide, for the first time, evidence of semiconducting properties on a hybridized (known traditionally as "semimetallic") InAs/GaSb composite quantum well (CQW). The positive energy gap results from either the size-quantization effect in thin CQWs or the hybridization effect in thick CQWs. In addition, we find that the hybridized CQW undergoes a semiconductor-to-semimetal transition when an in-plane magnetic field is applied.

The detailed sample structures and the fabrication processes are described elsewhere [10]. The sample parameters and the energy band diagrams are shown in Table I and the insets of Figs. 1 and 2, respectively. Here the $k = 0$ subband energies are calculated with the envelope-function approximation under a four-band $k \cdot p$ model [11]. The main focus of this paper is on the hybridized CQW, while the semiconducting sample is used for reference. These two samples represent two classes of subband alignments in the InAs/GaSb system. For the hybridized CQW, the lowest heavy-hole subband (HH_0) lies above the lowest electron subband (E_0), which was regarded as the only prerequisite of a semimetal in the past. In contrast, for the semiconducting CQW, HH_0 is below E_0, and it has an unambiguous positive band gap.

In order to investigate the relative position between the Fermi level (E_f) and subband levels at different front gate voltage (V_g), we carried out the capacitance-voltage (C-V) and Hall measurements at 4.2 K, and the results are plotted in Figs. 1 and 2. For the semiconducting sample in the V_g range from 10 V to -10 V, the Hall resistivity depends linearly on the perpendicular magnetic field ($B_\perp$) before the emergence of the quantum Hall plateaus. The linearity of Hall resistivity implies a single-particle transport, i.e., two-dimensional (2D) electrons never coexist with 2D holes in the semiconducting sample. The electron density, obtained from Hall measurements and plotted in Fig. 1(b), is 1.93×10^{12} cm^{-2} at $V_g = 10$ V and decreases linearly to 7.2×10^{11} cm^{-2} at $V_g = 0$ V. The electron channel switches to a hole channel in the vicinity of $V_g = -6$ V, and the hole density is determined to be 5.3×10^{11} cm^{-2} at $V_g = -10$ V. For C-V measurements, there are four components [12] that contribute to the measured capacitance per unit area (C_m) for our sample structure, i.e.,

$$\frac{1}{C_m} = \frac{1}{C_{\rm ox}} + \frac{d}{\varepsilon_{\rm AlSb}} + \frac{\langle z_0 \rangle}{\varepsilon_{\rm CQW}} + \frac{1}{e^2 D(E)},$$

where $C_{\rm ox}$ is the oxide dielectric capacitance per unit area, $\varepsilon_{\rm AlSb}$ and d are the dielectric constant and thickness of AlSb, respectively. In addition, $\varepsilon_{\rm CQW}$ and $\langle z_0 \rangle$ are the average dielectric constant and average position of the electrons in the CQW, and $D(E)$ is the 2D density of state (DOS). For an ideal two-dimensional system, the DOS is constant for one subband and dependent upon the effective mass m^*, i.e., $D(E) = m^*/\pi\hbar^2$. Figure 1(a) shows the normalized capacitance measured at 10 kHz with a 50 mV peak-to-peak ac signal for the semiconducting sample. It is found that C_m is featureless for $-4 < V_g \leq 10$ V when E_f is above E_0. Owing to the low density of the localized and interface states within the forbidden gap, C_m displays a dip when E_f is passing through the band gap from E_0 to HH_0, i.e., when V_g is biased from -5 V to -7 V. When the heavy-hole channel is fully turned on, C_m recovers to a slightly higher value. This small increase is, though in part due to the additional DOS of the heavy-hole subband, mainly from the reduction

TABLE I. Sample parameters. HH_0 is the lowest heavy-hole subband energy below the GaSb valence band maximum, E_{GaSb}, and E_0 is the lowest electron subband energy above the InAs conduction band minimum, E_{InAs}. The subband energy difference, ΔE_{sub}, is estimated by assuming that E_{GaSb} is 150 meV above E_{InAs}.

Sample	GaSb	InAs	HH_0	E_0	ΔE_{sub}
Semiconducting	60 Å	60 Å	21.5 meV	214 meV	85.5 meV
Hybridized	40 Å	140 Å	39.5 meV	68 meV	−42.5 meV

of $\langle z_0 \rangle$. This reduction occurs because the GaSb QW is a few tens of angstroms closer to the front gate than the InAs QW. This is confirmed by performing the C-V measurement on a sample with the InAs QW closer to the surface than the GaSb QW.

For the hybridized CQW, the C-V curve has new features. The step at $V_g \sim 5$ V in Fig. 2(a) results from the increase of DOS, and indicates the alignment of E_f and the second electron subband E_1. This identification of the capacitance signal at $V_g \sim 5$ V is confirmed by the Hall measurement. In the range of positive V_g, only 2D electrons are present in the CQW, and the Hall resistivity depends linearly on $B_\perp$ at low fields ($B_\perp < 1$ T). However, the longitudinal resistivity shows beating phenomena on the Shubnikov–de Haas oscillations when $V_g > 5$ V, indicating the occupation of the second electron subband. The total 2D electron density varies linearly from 2.6×10^{12} cm^{-2} at $V_g = 10$ V to 8.0×10^{11} cm^{-2} at $V_g = 0$ V. The linear dependence of the net carrier density on the gate voltage is consistent with the simple capacitor model. That is, $C_m \Delta V_g = \Delta Q$, where ΔQ is the net charge changed within ΔV_g. The dependence of density on the V_g for the hybridized sample is stronger, i.e., a larger C_m, than for the semiconducting sample due to a thinner oxide; 1300 Å compared to 2000 Å. In contrast, in the negative gate biases, $-10 \leq V_g < -1$ V, the Hall measurements (not shown) for the hybridized sample indicate a multiple-carrier transport. It is known that in the case of multiple-particle transport, the slope of Hall resistivity at high enough field is determined by the net carrier concentration, regardless of the mobility of the individual particle [13]. Consequently, the difference of the 2D hole and 2D electron density can be obtained and is plotted in Fig. 2(b). It is found that the hole density exceeds the electron density when $V_g < -4$ V. In this negative bias range, the capacitance reveals three pieces of information. First, in the vicinity of $V_g = -1$ V, the E_f is aligned with HH_0. The ~2% increase of C_m marks the onset of hole channel. Second, the most important feature is observed at $V_g \sim -4$ V, i.e., when electron and hole densities are equal.

The small dip of C_m is a direct result of the formation of a small energy gap by the coupling of in-plane dispersions of heavy hole and electron subbands. As illustrated in the following, the dashed curves in Figs. 3(a) and 3(b) are, respectively, the DOS and in-plane dispersions under a nonhybridized picture, assuming the HH_0 is 50 meV above the E_0, i.e., a semimetal with $E_g = -50$ meV. Here electron mass and hole mass are assumed to be $m_e^* = 0.03\ m_0$ and $m_h^* = 0.37\ m_0$, respectively [8]. This nonhybridized dispersion is valid when the

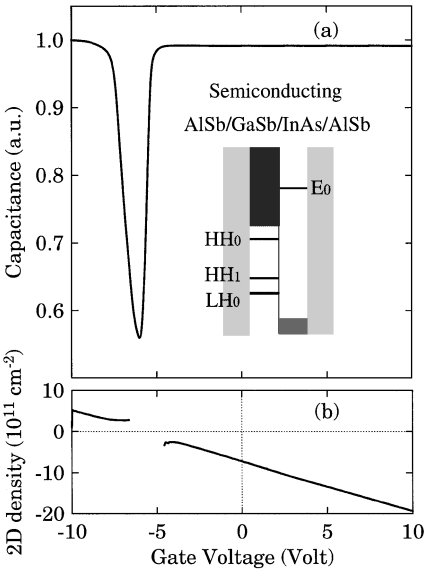

FIG. 1. (a) The normalized capacitance as a function of gate voltage for the semiconducting sample. The inset shows the energy diagram. (b) The *total* 2D density determined by the Hall measurements.

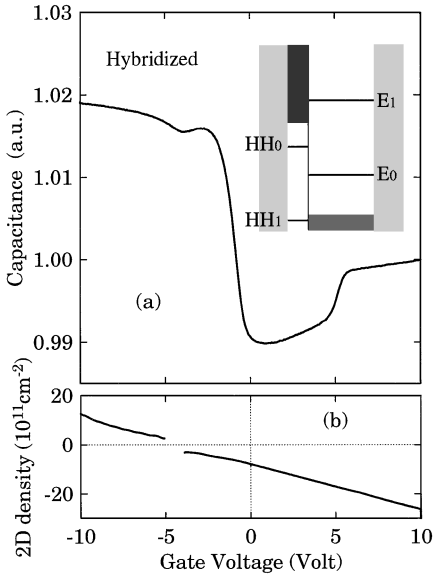

FIG. 2. (a) The normalized capacitance vs V_g for the hybridized sample. The inset shows the energy diagram. (b) The *net* 2D density obtained from the slope of the Hall resistivity.

GaSb and the InAs QW's are far separated. However, when these two wells are adjacent to each other, the degeneracy around the crossover is lifted due to the $k \cdot p$ interaction between electrons in the InAs and holes in the GaSb [3,5]. When the hybridization effect is considered, this conventionally recognized semimetal becomes a semiconductor with a W-shaped (or M-shaped) conduction (or valence) band dispersion, shown as solid curves in Fig. 3(b). The hybridization gap depends upon the coupling coefficient, which is determined by the degree of wave function overlap of the electrons in the InAs QW and the holes in the GaSb QW. Here we have chosen a coupling coefficient of 5 meV [3–5]. As a result of hybridization, the DOS is also changed. We find zero DOS within the hybridization gap as expected, and two van Hove singularities at the band edges [see solid curve in Fig. 3(a)]. However, due to the sample imperfections, the sharp feature of the DOS is smeared out significantly by the inhomogeneous broadening [14]. In other words, the resulting DOS after considering the hybridization and inhomogeneous broadening effects is closer to the dashed line in Fig. 3(a), but *with localized states within the hybridized gap.* As a result, this modification of DOS is reflected as a dip in C_m. Third, in the range $-10 \leq V_g < -5$ V, the C_m shows no features, implying that E_f is still above E_0 at $V_g = -10$ V. This is consistent with the Hall measurements and the fact that the DOS of a hole subband is more than ten times larger than that of an electron subband.

We have shown, so far, not only that both quantum Hall and C-V measurements confirm the coexistence of 2D electrons and 2D holes for the hybridized sample when $-10 \leq V_g < -1$ V, but also that there is a signature of hybridization gap on C_m at $V_g \sim -4$ V. In addition to the C-V curve, the transfer characteristics are more strongly influenced by the band hybridization. Figure 4(a) shows the typical I-V curve for the narrow gap semiconducting sample. For $V_g > -6$ V, the drain current (I_{DS}) is carried by 2D electrons in the InAs well, and the sample behaves as a conventional n-type field-effect transistor (FET). The I_{DS} turns on sharply from -6 V to -5 V, and increases monotonically as V_g is increased. Eventually, it reaches a saturation value of ~ 70 μA. By the same token, the sample is like a p-type FET in the voltage range $V_g < -6$ V. However, the saturation value for p channel is expected to be smaller due to two factors. One is because the hole mobility in the GaSb QW is 1 order of magnitude smaller than the electron mobility in the InAs QW. The other is because of a resistive tunneling process between the ohmic contacts and the hole channel [10]. That is, the channel conduction for $V_g < -6$ V is carried by electrons tunneling from the source region of the InAs QW to the GaSb QW and then tunneling back to the drain region of the InAs QW. When we superimpose transfer characteristics of n and p FET, we expect an asymmetric V-shaped I-V curve as observed for the semiconducting sample, where the hole channel is not turned on until the electron channel is turned off. The minimum of the V shape is a consequence of the Fermi level residing in the band gap, and it marks the onset of the switching between electron and hole conduction. On the other hand, in the case of a true semimetal system, the hole channel is turned on *before* the electron channel is turned off. The resulting transfer characteristic is then expected to be steplike, instead of V shaped, because there is no forbidden energy gap. However, this is not observed for the hybridized sample. In the voltage range $-10 \leq V_g < 0$ V, we still observed a V-shaped curve, a characteristic of a semiconducting sample. This result further confirms the existence of an energy gap when E_f lies between HH_0 and E_0.

Although both the semiconducting and the hybridized CQW exhibit an energy gap, they show distinct transport properties under a parallel magnetic field ($B_{\|}$), due to differences in the original mechanisms of the energy gap formation. In the presence of $B_{\|}$ applied along the y axis, electrons in the InAs well with in-plane momentum (k_x, k_y) will couple to holes in the GaSb well with

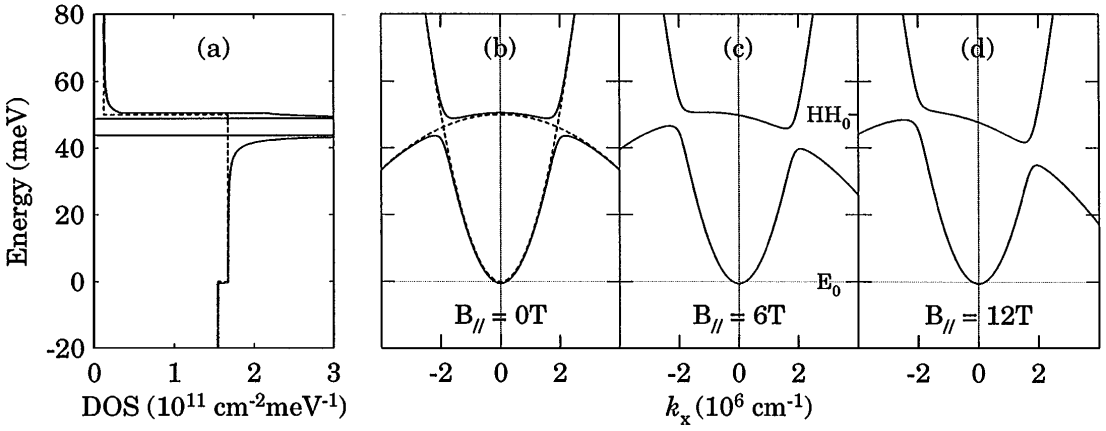

FIG. 3. (a) The density of states and (b) the in-plane dispersion relations of electrons in InAs and holes in GaSb without (dashed curve) and with (solid curve) consideration of the hybridization effect. (c), (d) The in-plane dispersions including the hybridization effect under a parallel magnetic field. Here the HH_0 is assumed to be 50 meV above the E_0.

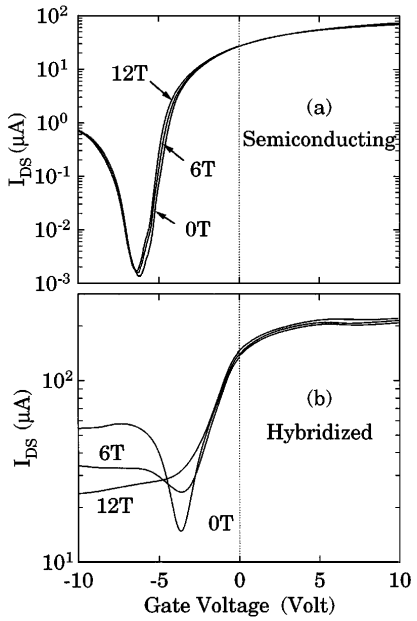

FIG. 4. The transfer characteristics under different in-plane magnetic fields for (a) the semiconducting and (b) the hybridized samples. The source-to-drain voltage is 0.1 V.

in-plane momentum $(k_x + eB_{\|}\langle z\rangle/\hbar, k_y)$ [15]. Here we chose the z axis as the growth direction, and $\langle z\rangle$ is about a one-half thickness of the CQW, i.e., 90 Å for the hybridized sample. In other words, a $B_{\|}$ causes a momentum displacement along k_x for the hole subband relative to the electron subband, but has no effect on the dispersion along k_y. Figures 3(c) and 3(d) plot the relative dispersions under two different $B_{\|}$. It is found that these two parabolas can be separated far enough to undergo a semiconductor-to-semimetal transition near 6 T. The transfer characteristics for the hybridized CQW under different $B_{\|}$ are shown in Fig. 4(b). While the V-shaped transfer characteristic weakens by 6 T, it is clear that, at $B_{\|} = 12$ T, the I-V curve turns into a steplike one, as expected for a true semimetal. In contrast, the $B_{\|}$ has hardly any effect on the semiconducting sample, as shown in Fig. 4(a).

The parallel-magnetic-field transport provides strong evidence of the formation of the hybridization gap due to the coupling of the electrons in the InAs QW and the holes in the GaSb QW. Based on the C-V and I-V characteristics of the hybridized sample, the hybridization energy gap can be estimated. As discussed earlier, due to the inhomogeneous broadening, the final DOS for this hybridization sample is close to the dashed curve shown in Fig. 3(a) with localized states within the hybridization gap, according to our C-V measurements. As is well known, localized electrons cannot contribute to the drain current. And, consequently, when the Fermi level is brought from extended states to these localized states, the drain current is reduced. As shown in Fig. 4(b), the V-shaped I-V curve extends over a voltage range of 4 V or so, which implies a total density of localized states of $C_m\Delta V_g/q = \Delta Q/q = 7.2 \times 10^{11}$ cm^{-2}. A simple estimate of the hybridization gap based on the constant 2D DOS [i.e., $D(E) = (m_e^* + m_h^*)/\pi\hbar = 1.7 \times 10^{11}$ cm^{-2} meV^{-1}] is 4 meV, consistent with the calculation [3–5].

In summary, we have carried out a complete and systematic study of InAs/GaSb systems, and demonstrated the formation of a positive band gap as a result of hybridization when the electron parabola overlaps with the hole. Owing to the nature of different mechanisms of the positive band gap formation, the hybridized system undergoes a semiconductor-to-semimetal transition when a parallel magnetic field is applied, while the semiconducting InAs/GaSb system shows transport properties independent of $B_{\|}$.

The work at NRL is supported by the Office of Naval Research, and the work at the University of Maryland is supported by the Joint Program for Advanced Electronic Materials and the Laboratory for Physical Sciences.

[1] L. L. Chang, in *Molecular Beam Epitaxy and Heterostructures*, edited by L. L. Chang and K. Ploog, NATO ASI Series E, Vol. 87 (Nijhoff, Dordrecht, 1985), p. 461.
[2] Because of a larger effective mass in the GaSb valence band, the heavy-hole subband energy is not as important as the electron subband energy in InAs in determining the energy band gap [G. A. Sai-Halasz, L. Esaki, and W. A. Harrison, Phys. Rev. B **18**, 2812 (1978)].
[3] M. Altarelli, Phys. Rev. B **28**, 842 (1983); A. Fasolino and M. Altarelli, Surf. Sci. **142**, 322 (1984); M. Altarelli, J. C. Maan, L. L. Chang and L. Esaki, Phys. Rev. B **35**, 9867 (1987).
[4] Y. Naveh and B. Laikhtman, Appl. Phys. Lett. **66**, 1980 (1995); Phys. Rev. Lett. **77**, 900 (1996).
[5] J. J. Quinn and J. J. Quinn, Surf. Sci. **361-362**, 930 (1996).
[6] L. M. Claessen, J. C. Maan, M. Altarelli, P. Wyder, L. L. Chang, and L. Esaki, Phys. Rev. Lett. **57**, 2556 (1986).
[7] J. Kono, B. D. McCombe, J. P. Cheng, I. Lo, W. C. Mitchel, and C. E. Stutz, Inst. Phys. Conf. Ser. **144**, 292 (1996); Phys. Rev. B **55**, 1617 (1997).
[8] R. J. Wagner, B. V. Shanabrook, M. J. Yang, and J. R. Waterman, Superlattices Microstruct. **21**, 95 (1997).
[9] R. J. Nicholas, M. van der Burgt, M. S. Daly, K. S. H. Dalton, M. Lakrimi, N. J. Mason, D. M. Symons, P. J. Walker, R. J. Warburton, D. J. Barnes, and N. Miura, Physica (Amsterdam) **201B**, 271 (1994).
[10] M. J. Yang, Fu-Cheng Wang, C. H. Yang, B. R. Bennett, and T. Q. Do, Appl. Phys. Lett. **69**, 85 (1996).
[11] G. Bastard, Phys. Rev. B **25**, 7584 (1982).
[12] T. P. Smith III, W. I. Wang, and P. J. Stile, Phys. Rev. B **34**, 2995 (1986).
[13] See, e.g., *Semiconductors*, edited by R. A. Smith (Cambridge University Press, New York, 1978), p. 113.
[14] For example, a one-monolayer deviation on the InAs (or GaSb) QW results in an E_0 (or HH_0) variation of 2 meV (or 5 meV).
[15] K. K. Choi, B. F. Levine, N. Jarosik, J. Walker, and R. Malik, Phys. Rev. B **38**, 12 362 (1988).